ARTICLE OPEN

Check for updates

Arsenic trioxide and p97 inhibitor synergize against acute myeloid leukemia by targeting nascent polypeptides and activating the ZAKα–JNK pathway

Shufeng Xie[1,7✉], Hui Liu[2,7], Shouhai Zhu[3,7], Zhihong Chen[1,7], Ruiheng Wang[1], Wenjie Zhang[4], Huajian Xian[1], Rufang Xiang[1,5], Xiaoli Xia[1], Yong Sun[1], Jinlan Long[4], Yuanli Wang[6], Minghui Wang[1], Yixin Wang[1], Yaoyifu Yu[1], Zixuan Huang[1], Chaoqun Lu[1], Zhenshu Xu[4✉] and Han Liu[1✉]

Arsenic trioxide (ATO) has exhibited remarkable efficacy in treating acute promyelocytic leukemia (APL), primarily through promoting the degradation of the PML-RARα fusion protein. However, ATO alone fails to confer any survival benefit to non-APL acute myeloid leukemia (AML) patients and exhibits limited efficacy when used in combination with other agents. Here, we explored the general toxicity mechanisms of ATO in APL and potential drugs that could be combined with ATO to exhibit synergistic lethal effects on other AML. We demonstrated that PML-RARα degradation and ROS upregulation were insufficient to cause APL cell death. Based on the protein synthesis of different AML cells and their sensitivity to ATO, we established a correlation between ATO-induced cell death and protein synthesis. Our findings indicated that ATO induced cell death by damaging nascent polypeptides and causing ribosome stalling, accompanied by the activation of the ZAKα-JNK pathway. Furthermore, ATO-induced stress activated the GCN2–ATF4 pathway, and ribosome-associated quality control cleared damaged proteins with the assistance of p97. Importantly, our data revealed that inhibiting p97 enhanced the effectiveness of ATO in killing AML cells. These explorations paved the way for identifying optimal synthetic lethal drugs to enhance ATO treatment on non-APL AML.

Cancer Gene Therapy (2024) 31:1486–1497; https://doi.org/10.1038/s41417-024-00818-z

INTRODUCTION

Acute myeloid leukemia (AML) is a heterogeneous hematological malignancy characterized by the infiltration of abnormal and differentiated cells into the bone marrow and blood [1]. Acute promyelocytic leukemia (APL) represents 5–10% of AML, which can be cured through All-trans retinoic acid and arsenic trioxide (ATO) combination treatment [2–6]. However, ATO alone fails to confer any survival benefit to non-APL AML patients and exhibits limited efficacy when used in combination with other agents [7–10]. To broaden the successful application of ATO in APL to other AML, a deeper exploration into the general mechanisms of ATO in APL is imperative. This exploration will pave the way for identifying optimal synthetic lethal drugs to enhance treatment outcomes.

The main mechanism of ATO inducing APL remission is to promote the degradation of the PML-RARα fusion protein [11–15]. In addition, ATO has the capacity to induce reactive oxygen species (ROS) [16, 17], contributing to cell death. Nevertheless, studies have indicated that ROS might not be indispensable for ATO-induced cell death [18]. Thus, whether PML-RARα degradation and ROS upregulation are sufficient to cause APL cell death remains to be explored. Furthermore, ATO directly targets certain functional proteins containing sulfhydryl groups, suggesting another pathway leading to cell apoptosis [19, 20]. Hence, we propose that the general mechanism of ATO-induced APL cell death is associated with protein damage. The accumulation of damaged proteins in the endoplasmic reticulum (ER) can cause ER stress [21]. To manage mild stress and maintain cellular homeostasis, cells initiate the unfolded protein response (UPR), which encompasses three pathways: PERK–eIF2α, IRE1α-XBP1, and ATF6α [22, 23]. However, severe ER stress triggers cell apoptosis, primarily through the activation of the PERK–eIF2α–ATF4–CHOP pathway [23–25], which is also one part of the integrated stress response (ISR). The ISR involves four serine/threonine kinases: PERK, PKR, HRI, and GCN2 [26, 27]. Among these, GCN2 can be activated by free uncharged tRNAs [28], ribosome collisions [29], or ribosome stalling [30]. Arsenic has been demonstrated to induce apoptosis in various cells through abnormal ER stress or UPR [31–35].

[1]Shanghai Institute of Hematology, State Key Laboratory of Medical Genomics, National Research Center for Translational Medicine at Shanghai, Ruijin Hospital, Shanghai Jiao Tong University School of Medicine and School of Life Sciences and Biotechnology, Shanghai, China. [2]Key Laboratory of Pediatric Hematology & Oncology of the Ministry of Health of China, Department of Hematology & Oncology, Shanghai Children's Medical Center, School of Medicine, Shanghai Jiao Tong University, Shanghai, China. [3]Department of Oncology, Mayo Clinic, Rochester, MN, USA. [4]Fujian Institute of Hematology, Fujian Provincial Key Laboratory on Hematology, Fujian Medical University Union Hospital, Fuzhou, China. [5]Department of General Practice, Ruijin Hospital, Shanghai Jiao Tong University School of Medicine, Shanghai, China. [6]Department of Hematology, Jingzhou Hospital Affiliated to Yangtze University, Jingzhou, Hubei, China. [7]These authors contributed equally: Shufeng Xie, Hui Liu, Shouhai Zhu, Zhihong Chen.
✉email: xieshufeng@sjtu.edu.cn; zhenshuxu@yahoo.com; liuhan68@sjtu.edu.cn

Received: 28 February 2024 Revised: 25 July 2024 Accepted: 29 July 2024
Published online: 9 August 2024

Nevertheless, limited attention has been devoted to exploring the ISR induced by ATO. Therefore, it holds great significance to investigate whether ATO-induced protein damage activates ISR or UPR in APL cells.

Proteins that have undergone irreversible damage necessitate clearance through a protein degradation system [36], comprising ER-associated degradation (ERAD) [37] and ribosome-associated quality control (RQC) [38]. The ERAD substrates are translocated from the ER membrane to the cytosol with the assistance of HRD1, a process coupled to energy derived from ATP hydrolysis by the AAA ATPase VCP/p97 [39]. RQC is a pathway targeting defective nascent peptides on stalled ribosomes. Key proteins in this pathway include the ubiquitin ligase Listerin and its cofactor NEMF. NEMF recognizes the peptidyl−transfer RNA molecules and recruits Listerin to ubiquitinate the stalled polypeptides, subsequently extracting them from the 60 S ribosome with the aid of VCP/p97 [40–42]. Ultimately, substrates from both pathways undergo degradation by the proteasome. Considering the pivotal role of VCP/p97 in ERAD and RQC, exploration of p97 inhibitors as potential synthetic lethal drugs with ATO for treating non-APL AML is warranted.

In this study, we determined that PML-RARα degradation and ROS upregulation were insufficient to cause APL cell death. We further illustrated that ATO could cause nascent polypeptides damage and ribosome stalling, accompanied by the activation of the GCN2–ATF4 mediated ISR and the ZAKα–JNK pathway. Furthermore, the damaged proteins were degraded by RQC. Significantly, our findings unveiled synthetic lethal effects between ATO and p97 inhibitors in ATO-low-sensitive AML cells. These discoveries lay a foundation for advancing the application of ATO in clinical settings.

MATERIALS AND METHODS

Chemicals

Arsenic trioxide, N-acetyl-L-cysteine and H_2O_2 (Sigma, St Louis, MO, USA); Glutathione, DCFH-DA (Beyotime Biotechnology, Shanghai, China); CCK-8, GCN2iB, NMS873, JNK-IN-8 (Topscience, Shanghai, China); Anisomycin, puromycin, rapamycin, cycloheximide, thapsigargin, tunicamycin, 4EGI-1 (MedChemExpress, Monmouth, NJ, USA); GSK2656157 (Selleck, Houston, TX, USA).

Cell lines and cell culture

Human AML leukemia cell lines NB4, MV4-11, NOMO-1, MOLM-13, THP-1, U937, HL-60, and Kasumi-1 were purchased from DSMZ. Cells were cultured in RPMI 1640 containing 10% FBS, at 37 °C with 5% CO_2. NB4-AR (ATO-resistant) cell line was generated by continuously treating NB4 cells with a sublethal dose of ATO (1 μM) for over 4 weeks. The cell lines had been identified by STR profiling. Mycoplasma testing was performed and no contamination was observed.

Cell survival viability and apoptosis

Cell viability was analyzed using the CCK-8. The apoptosis was performed using the Annexin V-APC or Annexin V-Pacific Blue Apoptosis Detection Kit (Biolegend, CA, USA). Data produced by the flow cytometer were analyzed using the FlowJo software.

Immunoblots

Rabbit against human antibodies PML (ab72137) (Abcam, Cambridge, UK), p-eIF2α (44-728G) (Life Technologies, Carlsbad, CA, USA), ATF4 (sc-200) (Santa Cruz, Dallas, TX, USA), XBP1s (12782S), p-JNK (4668P), and eIF2α (5324S) (Cell Signaling Technology, Danvers, MA, USA), NEMF (11840-1-AP), ATF6 (24169-1-AP) and HRD1 (13473-1-AP) (Proteintech, Rosemont, IL, USA), JNK (A4867), RPS2 (A6728) and p97 (A13368) (ABclonal Technology, Wuhan, China), ZAKα (A301-993A) (Bethyl Laboratories, Montgomery, TX, USA). Mouse against human antibodies GAPDH (AC002) and β-Actin (AC004) (ABclonal Technology), Ubiquitin (PA1-187) (Life Technologies), Puromycin (MABE343) (Millipore, Boston, MA, USA), BiP (610978) (BD Biosciences, San Jose, CA, USA). Immunoblot signals were acquired with the Amersham Imager 600 (General Electric Company, Boston, MA, USA).

RNA-seq analysis

The mRNA-Seq library was constructed and sequenced using the Illumina TruSeq library construction kit and BGISEQ-500 PE100 (BGI Technology Service, Wuhan, China). Differentially expressed genes were selected based on $|\log2FoldChange| > 1$ and P value < 0.05.

Aggresome and global protein synthesis detection

Protein aggresome detected by Enzo PROTEOSTAT® Aggresome detection kit (Enzo Life Sciences, Farmingdale, NY, USA) following flow cytometer. The global protein synthesis rate was detected by Click-iT™ Plus OPP Alexa Fluor™ 647 Protein Synthesis Assay Kit or Click-iT™ HPG Alexa Fluor™ 488 Protein Synthesis Assay Kit (Thermo Fisher Scientific, Rockford, IL, USA).

ROS measurement

NB4 cells were treated with ATO or H_2O_2 for the indicated time. And 10 μM DCFH-DA was added to detect the ROS level following recommendations. Data produced by the flow cytometer were analyzed using the FlowJo software.

qRT-PCR

RNA was isolated with Eastep® Super Total RNA Extraction Kit (Promega, Madison, WI, USA) and reverse-transcribed with the HiScript III 1st Strand cDNA Synthesis Kit (+gDNA wiper) (Vazyme, Nanjing, China). The collected cDNA was amplified using ChamQ SYBR Color qPCR Master Mix (Low ROX Premixed) (Vazyme). The relative fold expression values were determined by the ΔΔCt method and normalized to GAPDH as a reference gene. Primers: ATF4-F: GGCCAAGCACTTCAAACCTC, ATF4-R: GAGAAGGCATCCTCCTTGCTG; GAPDH-F: ACAACTTTGGTATCGTGGAAGG, GAPDH-R: GCCATCACGCCACAGTTTC.

Co-immunoprecipitation

In total, 1×10^7 NB4 Cells were treated with Biotin-As (Toronto Research Chemicals, Toronto, Canada) for 4 h and then 20 μM puromycin was added for another 30 min. Following treatment, the cells were rinsed once with PBS and lysed in lysis buffer (50 mM Tris-Cl [pH 7.4], 150 mM NaCl, 1% NP-40, 1 mM DTT, 0.25% sodium deoxycholate, phosphatase inhibitor cocktail, EDTA-free Protease inhibitor cocktail). Then streptavidin magnetic beads (MedChemExpress) or protein G (Thermo Fisher Scientific) were used to pull the target protein down following the described protocol.

Immunofluorescence

The NB4 cells were pre-treated with 0.1 μg/mL puromycin for 1 h, and then 4 μM Biotin-As was added for another 16 h. The cells were stained with anti-puromycin antibody, FITC-Streptavidin (Leinco Technologies, St. Louis, MO, USA), and Goat anti-Mouse IgG Secondary Antibody, DyLight™ 650 (Thermo Fisher Scientific) following recommendations. The aggresome in the cell was stained by the ProteoStat®Aggresome detection kit following recommendations. Subsequent operations were performed following the described protocol.

Polysome profiling

In all, 2×10^7 NB4 Cells were treated with 1.5 μM ATO for 6 h. Then the cells were rinsed once with PBS and lysed in lysis buffer (20 mM Tris-Cl [pH 8], 150 mM KCl, 15 mM $MgCl_2$, 1% Triton X-100, 1 mM DTT, phosphatase inhibitor cocktail [Epizymebiotech, Shanghai, China], EDTA-free Protease inhibitor cocktail [Epizymebiotech], 40 U/mL RNasin [Sango Biotech, Shanghai, China], 100 μg/mL cycloheximide). Lysates were run through 5–50% sucrose gradients (20 mM Tris-Cl [pH 8], 150 mM KCl, 15 mM $MgCl_2$, 1 mM DTT, 40 U/mL RNasin, 100 μg/mL cycloheximide) using Beckman Coulter SW41 Ti rotor at 40,000 rpm for 4 °C for 3 h. The absorbance at 260 nm of the gradients was recorded by using a Biocomp piston gradient fractionator.

Phosphorylated protein enrichment and detection

The cells were treated with an inhibitor for the indicated time. Then the cells were rinsed once with PBS and lysed in lysis buffer (50 mM Tris-Cl [pH 7.4], 150 mM NaCl, 1% NP-40, 1 mM DTT, 0.25% sodium deoxycholate, phosphatase inhibitor cocktail, EDTA-free Protease inhibitor cocktail). The phosphorylated proteins in the cell lysate were enriched by Phos-tag™ Agarose (NARD, Osaka Prefecture, Japan) following the described protocol. And p-ZAKα was detected by immunoblot.

Lentivirus-based knockdown

Target sequences p97-1 (CCTAGCCCTTATTGCATTGTT) and p97-2 (AGATCCGTCGAGATCACTTTG) against human p97, ZAKα-1 (TTCACTTCCCA CCACTAATTA) and ZAKα-2 (CCATTAAGTATCAACAGATTA) against human ZAKα and a control scrambled sequence (CCTAAGGTTAAGTCGCCCTCG) that has no significant homology with the human genome were inserted into the pLKO.1-mCherry vector, according to the manufacturer's protocol (Addgene, Watertown, MA, USA). A generated lentivirus carrying shRNA was used to infect target cells for 2 days, and the cells were subjected to puromycin selection.

Mouse studies

NSG mice were purchased from Vital River Laboratory. In all, 0.5×10^6 Luciferase-GFP-Kasumi-1 tumor cells were injected into NSG mice (6 weeks, female) intravenously. Mice were allocated randomly into different experimental groups (4 groups [vehicle, ATO, NMS873, ATO + NMS873], $n = 5$) and then intraperitoneally administered 2 mg/kg ATO or 2.6 mg/kg NMS873, respectively, or in combination, every other day for two weeks, beginning 14 days after the xenograft. Tumor growth was monitored by the quantitative imaging system. Mice were sacrificed by inhalation of CO_2 when they became moribund. Animal care and sacrifice were conducted according to methods approved by the Animal Care and Use Committee, the Center for Animal Experiments of Shanghai Jiao Tong University.

Statistical analysis

The two-tailed Student *t* test was used to analyze the differences between the control and experimental groups. The log-rank Kaplan–Meier survival test was used to compare the survival distributions of the different treatment groups in an AML xenograft mouse model. The statistically significance level is indicated as $^*P < 0.05$, $^{**}P < 0.01$, $^{***}P < 0.001$, or $^{****}P < 0.0001$. Error bars reflect ± SEM of three independent experiments.

RESULTS

PML-RARα degradation and ROS upregulation are insufficient to cause APL cell death

To assess whether PML-RARα degradation is adequate to trigger APL apoptosis, we exposed the NB4 cell line to varying concentrations of ATO. The results revealed that NB4 cells treated with 1.5 μM ATO for 24 h resulted in obvious apoptosis (Fig. 1A). Intriguingly, PML-RARα protein levels were significantly reduced under 0.2 μM ATO treatment for 12 h (Fig. 1B), indicating that PML-RARα degradation is insufficient for APL cell death.

In addition to PML-RARα degradation, ROS constitute another crucial mechanism in APL apoptosis [16, 17]. DCFH-DA was employed to detect ATO-induced ROS levels [43]. The NB4 cells were treated with different concentrations of ATO for 4 h and the results revealed an elevation in ROS levels after ATO treatment, with no significant difference observed among groups (Fig. 1C, D). Furthermore, NB4 cells treated with 10 or 20 μM H_2O_2 exhibited a similar ROS accumulation induced by a lethal dose of ATO, this ROS level failed to generate a corresponding apoptosis ratio (Fig. 1E–H). Hence, the elevated ROS levels induced by ATO were insufficient to induce cell apoptosis, aligning with previous findings [18].

In search of an additional mechanism explaining the sensitivity of APL cells to arsenic, an ATO-resistant strain of NB4 (NB4-AR) was constructed (Supplementary Fig. S1A). RNA-seq data revealed high expression of Defensin family proteins in NB4-AR cells, a class of cysteine-rich peptides (Supplementary Fig. S1B). Consequently, we hypothesize that arsenic primarily acts by targeting the sulfhydryl group of cysteine in proteins. To validate this hypothesis, the NB4 cells were pre-treated with sulfhydryl reagents N-acetyl-L-cysteine (NAC) or Glutathione (GSH) for 1 h, and then 2 μM ATO was added for another 24 h. Both reagents inhibited the death of NB4 cells caused by ATO (Fig. 1I). These results revealed the importance of cysteine in proteins as a critical target of arsenic attack.

The sensitivity of AML cells to ATO is related to protein synthesis

Consequently, we hypothesized that extensive protein damage plays a crucial role in ATO-induced cell death. We treated NB4 cells with 1 or 1.5 μM ATO for 16 h to detect ubiquitinated and aggregated proteins. The lethal dose of ATO significantly increased the level of ubiquitinated and aggregated proteins (Fig. 2A, B), indicating heightened protein damage. In contrast, treatment with 10 or 20 μM H_2O_2 failed to induce a comparable level of protein aggregation as observed with ATO (Fig. 2C), suggesting that APL cell apoptosis was associated with ATO-induced protein damage and was not solely mediated by ROS. The lethal dose of ATO disrupts proteostasis, and protein synthesis emerges as a pivotal factor influencing protein homeostasis [44]. Thus, we examined the protein synthesis of different AML cells and their sensitivity to ATO and found that cells with higher protein synthesis were more sensitive to ATO (Fig. 2D–F).

To further validate protein synthesis as a key target in arsenic-induced cell death, we employed various protein synthesis inhibitors to assess their impact on ATO toxicity. The effectiveness of these inhibitors in suppressing protein synthesis in NB4 cells was confirmed (Fig. 2G, H and Supplementary Fig. S2A). Then, the NB4 cells were pre-treated with different inhibitors for 1 h, and then 1.5 μM ATO was added for another 24 h. The results showed that cycloheximide (CHX) and 4EGI-1 can suppress ATO-induced apoptosis, whereas puromycin had the opposite effect, promoting apoptosis induced by ATO (Fig. 2I and Supplementary Fig. S2B). We further confirmed the protein synthesis inhibition of 0.2 μg/mL puromycin (Supplementary Fig. S2C). However, due to the high apoptosis ratio induced by 0.2 μg/mL puromycin, we employed lower concentrations (0.1 or 0.15 μg/mL) to treat NB4 cells. Interestingly, these concentrations improved the apoptosis ratio induced by 1 or 1.5 μM ATO (Supplementary Fig. S2D–F). The distinct impact of puromycin, CHX, and 4EGI-1 in the presence of ATO raised questions. We hypothesized that puromycin treatment may generate more nascent polypeptides for ATO to target, thereby causing increased protein damage, as puromycin can enter the ribosomal A-site and induce the release of peptidyl-puromycin products, commonly used as reagents for labeling nascent polypeptides [45].

ATO targets nascent polypeptides while activating the GCN2–ATF4 pathway

To investigate whether ATO induces protein damage by targeting nascent polypeptides, we conducted microscopy analysis. Utilizing biotinylated arsenic (Biotin-As), which mimics the effects of ATO [12], we found partial colocalization of puromycin-labeled nascent polypeptides with aggresome and Biotin-As, suggesting an interaction between arsenic and nascent polypeptides (Fig. 3A and Supplementary Fig. S3). Furthermore, immunoblot revealed that puromycin-labeled nascent polypeptides in the cell lysate could be pulled down with streptavidin magnetic beads after 1 μM Biotin-As treatment for 4 h, confirming the interaction between arsenic and nascent polypeptides (Fig. 3B).

Subsequently, we examined the stress induced by ATO on NB4 cells. Previous studies have indicated that arsenic can induce ER stress or UPR in various cell types [31–35]. Therefore, we investigated UPR activation under ATO treatment. We treated NB4 cells with 0.5 or 2 μM ATO for the indicated time and immunoblot analysis revealed that a lethal dose of ATO significantly increased the levels of p-eIF2α and ATF4 in NB4 cells after 4 h of treatment (Fig. 3C). This dramatic increase of ATF4 roused our interest. Thus, we detected the RNA level of ATF4 after ATO treatment, showing a slight increase in the mRNA level of ATF4 (Supplementary Fig. S4A). Therefore, the increased protein level of ATF4 was mainly due to the translation of ATF4 mRNA under stress [46]. We also detected the ATF4 level after treatment of 10 μM H_2O_2 for 4 h. The result showed that H_2O_2 treatment could not induce a dramatic increase of ATF4, which proved the difference between ATO and H_2O_2 again (Supplementary

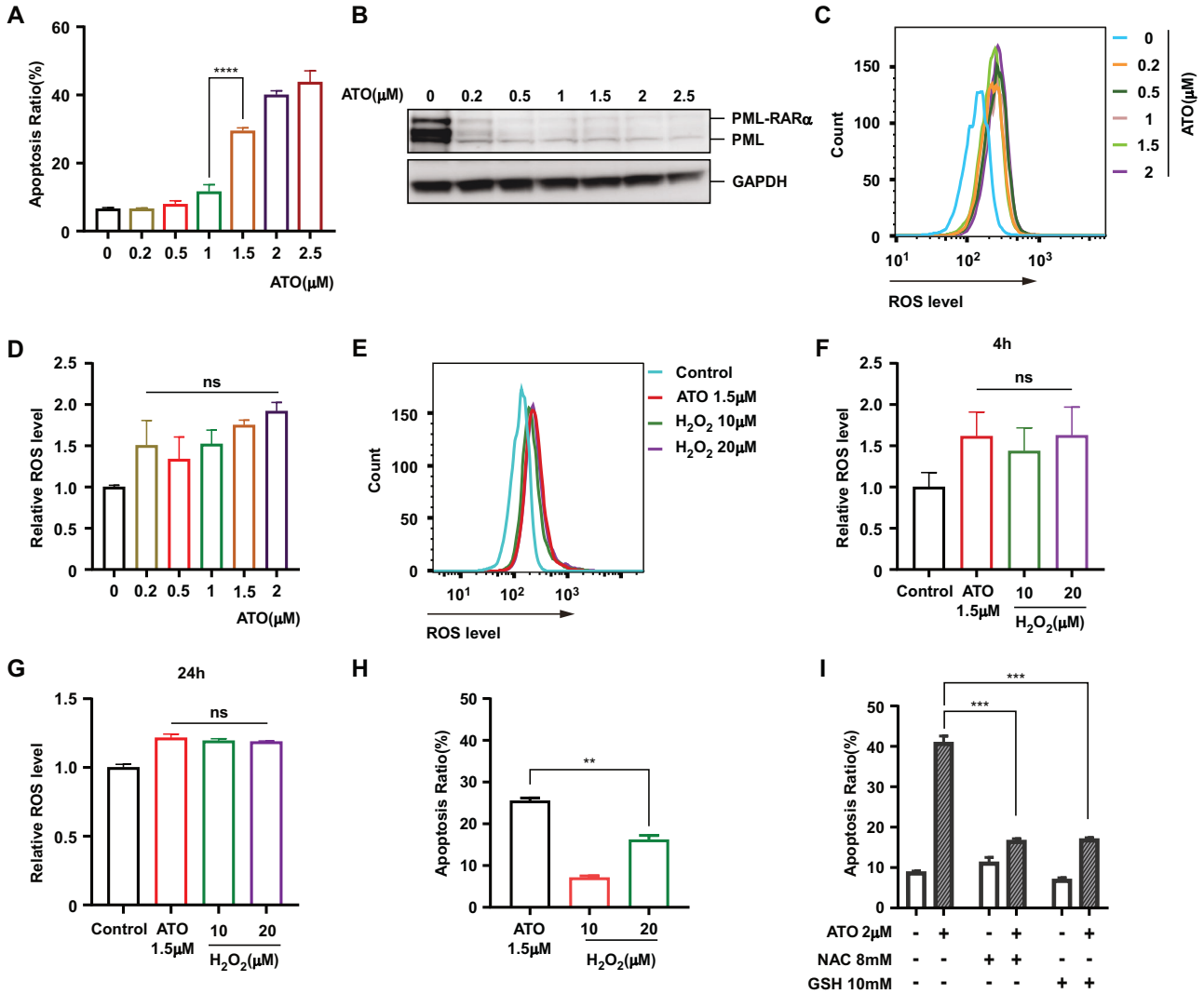

Fig. 1 PML-RARα degradation and ROS upregulation are insufficient to cause APL cell death. A NB4 cells were treated with different doses of ATO for 24 h, and apoptosis was detected by flow cytometry. **B** PML-RARα in the NB4 cells was detected by immunoblot after treating with different doses of ATO for 12 h. **C** ROS level in NB4 induced by ATO for 4 h was detected by using 10 μM DCFH-DA. **D** Quantification of ROS level in NB4 induced by ATO for 4 h. Normalized to control (0 μM ATO). **E** NB4 cells were treated with 1.5 μM ATO, 10 or 20 μM H_2O_2 for 4 h, and then ROS level was detected by using 10 μM DCFH-DA. **F** Quantification of ROS level in NB4 induced by 1.5 μM ATO, 10 or 20 μM H_2O_2 for 4 h. Normalized to control. **G** Quantification of ROS level in NB4 induced by 1.5 μM ATO, 10 or 20 μM H_2O_2 for 24 h. Normalized to control. **H** The apoptosis ratio of NB4 cells treated with 1.5 μM ATO or different doses of H_2O_2 for 24 h was detected by flow cytometry. **I** NB4 cells were pre-treated with 8 mM NAC or 10 mM GSH for 1 h, and then 2 μM ATO was added for another 24 h. Apoptosis was detected by flow cytometry. Two-tailed Student *t* test, $^{**}P < 0.01$, $^{***}P < 0.001$, $^{****}P < 0.0001$, the ns indicate no significant difference. Error bars reflect ± SEM of three independent experiments.

Fig. S4B). ATF6, XBP1s, and BiP—an ER chaperone aiding in protein refolding of misfolded proteins [47], were not activated by ATO treatment (Fig. 3C and Supplementary Fig. S5). The increase in ATF4 levels may result from the activation of PERK [22, 23] or GCN2 [26, 27]. To distinguish between PERK or GCN2 was activated by ATO treatment, we utilized a PERK inhibitor (PERKi, GSK2656157) or GCN2 inhibitor (GCN2iB) to pre-treat NB4 cells for 1 h, and then 2 μM ATO was added for another 4 h. The results showed that GCN2iB could inhibit the activation of ATF4 and p-eIF2α induced by ATO, while PERKi could not (Fig. 3D), suggesting that ATO-induced protein damage could activate the GCN2–ATF4 pathway.

ATO induces ribosome stalling and activates the ZAKα–JNK pathway

Our previous findings demonstrated that ATO-induced protein damage could activate the GCN2–ATF4 pathway. Research has shown that ribosome stalling triggers the JNK and GCN2-mediated stress response pathways [30, 48, 49]. Thus, we hypothesized that ATO could induce ribosome stalling to activate the GCN2–ATF4 pathway. To investigate this, we employed polysome profiling to examine translation behavior. The results demonstrated that upon 1.5 μM ATO treatment for 6 h, 80 S ribosomes increased while polysomes decreased (Fig. 4A and Supplementary Fig. S6), indicative of initiation ribosome stalling [50, 51]. Otherwise, we verified that the JNK pathway could be activated by a lethal dose of ATO treatment and that the JNK inhibitor could attenuate the apoptosis induced by ATO (Fig. 4B, C). These findings were in accord with the concept that ribosome stalling activates the JNK [48, 49] and JNK activation is a mediator of ATO-induced apoptosis in APL cells [52]. In addition, ZAKα is essential for ribosome stalling-induced JNK activation [48, 49]. Phos-tag™ Agarose was used to enrich phosphorylated proteins, revealing that the lethal dose of ATO triggered rapid activation of ZAKα and was sustained during extended treatment. Conversely, nonlethal dose of ATO

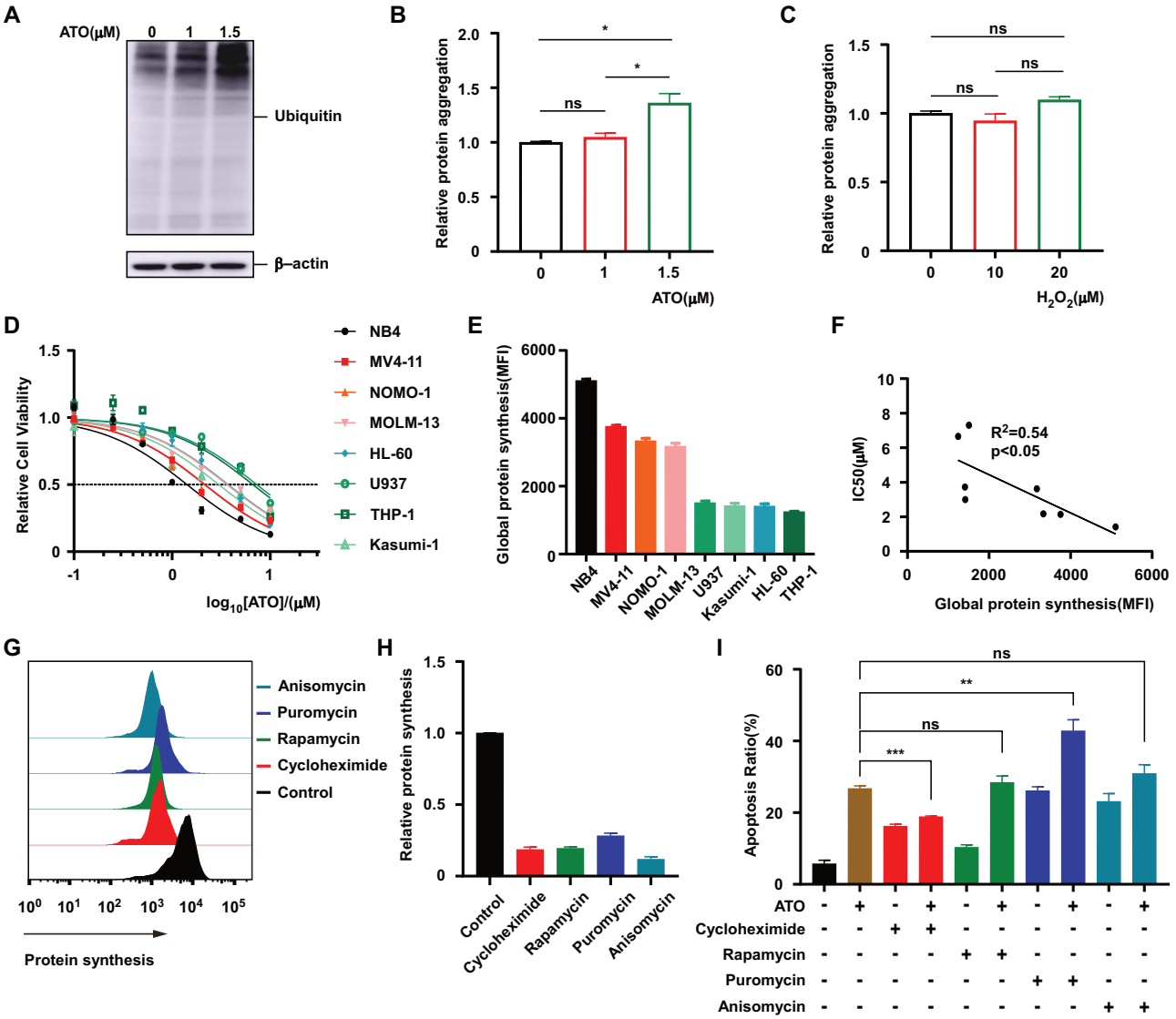

Fig. 2 The sensitivity of AML cells to ATO is related to protein synthesis. A Ubiquitinated proteins were detected by immunoblot after treatment with 1 or 1.5 μM ATO for 16 h. **B**, **C** ProteoStat kit was used to detect protein aggregates in NB4 cells by flow cytometry after treatment with 1 or 1.5 μM ATO (**B**) or 10 or 20 μM H_2O_2 (**C**) for 16 h. Normalized to control. **D** Cell viability of indicated AML cell lines with ATO treatment after 24 h. **E** The global protein synthesis of indicated AML cell lines was detected by Click-iT™ Plus OPP Alexa Fluor™ 647 Protein Synthesis Assay Kit. **F** Correlation between global protein synthesis and IC_{50}. **G** The global protein synthesis of NB4 cells treated with 0.25 μg/mL cycloheximide, 25 μM rapamycin, 0.2 μg/mL puromycin, or 100 nM anisomycin for 20 h was detected by Click-iT™ HPG Alexa Fluor™ 488 Protein Synthesis Assay Kit. **H** Quantification of global protein synthesis (Click-iT™ HPG Alexa Fluor™ 488 Protein Synthesis Assay Kit) in NB4 treated with indicated protein synthesis inhibitors for 20 h. Normalized to control. **I** NB4 cells were pre-treated with 0.25 μg/mL cycloheximide, 25 μM rapamycin, 0.2 μg/mL puromycin, or 100 nM anisomycin for 1 h, and then 1.5 μM ATO was added for another 24 h. Apoptosis was detected by flow cytometry. Two-tailed Student *t* test, $^{*}P < 0.05$, $^{**}P < 0.01$, $^{***}P < 0.001$, the ns indicate no significant difference. Error bars reflect ± SEM of three independent experiments.

activated ZAKα after prolonged exposure, suggesting that the lethal dose of ATO results in more severe ribosome stalling than the nonlethal dose (Fig. 4D). Notably, activation of ATF4, but not JNK was observed in NB4 cells treated with the nonlethal dose of ATO (Figs. 3C and 4B), indicating that only the nonlethal dose of ATO induces mild ribosome stalling that cannot activate JNK. Furthermore, we confirmed that ZAKα knockdown could decrease ATO-induced apoptosis (Fig. 4E, F), suggesting the importance of ZAKα in apoptosis induced by ATO.

NMS873 enhances the sensitivity of APL to ATO

To further investigate whether ATO-induced damaged proteins are processed through RQC or ERAD, we examined the interaction between arsenic and RQC- or ERAD-associated proteins in NB4. The results showed that NEMF (RQC-associated protein) [42] in the cell lysate could be pulled down with streptavidin magnetic beads, but not HRD1 (ERAD-associated protein) [39], after 1 μM Biotin-As treatment for 4 h, suggesting that ATO-induced damaged proteins were handled through RQC (Fig. 4G). Previous studies showed that p97 was an important protein in RQC [41, 53]. Therefore, we explored the interaction between p97 and NEMF in NB4. The NB4 cells were treated with 1 μM Biotin-As for 4 h, and then 20 μM puromycin was added for another 30 min. The results showed that the puromycin-labeled nascent polypeptides and p97 could be pulled down with protein G-linked NEMF antibody (Fig. 4H). Furthermore, more puromycin-labeled nascent polypeptides and p97 were pulled down in the Biotin-As treated group compared with the

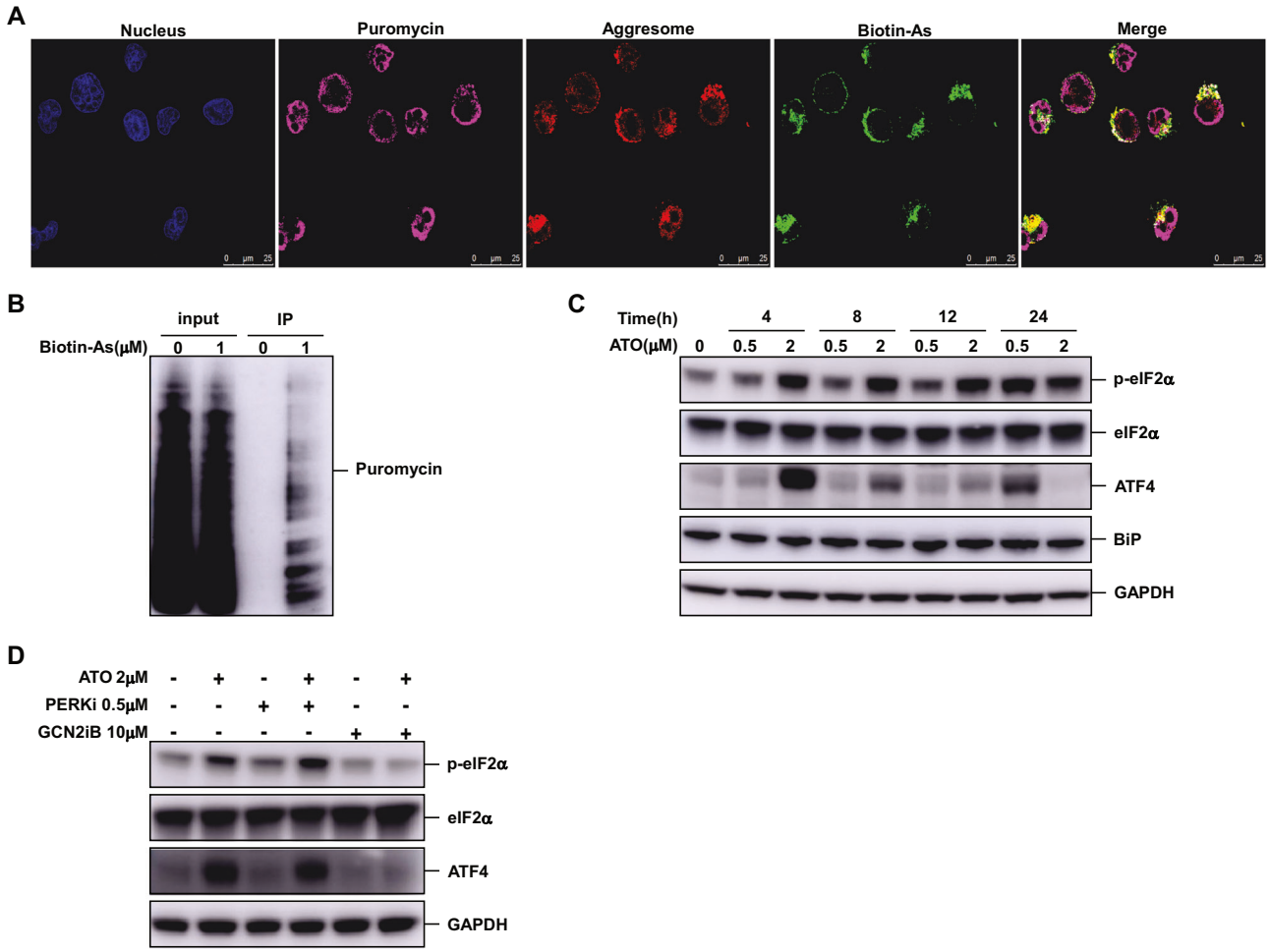

Fig. 3 ATO targets nascent polypeptides while activating the GCN2–ATF4 pathway. A The NB4 cells were pre-treated with 0.1 μg/mL puromycin for 1 h, and then 4 μM Biotin-As was added for another 16 h. Immunofluorescence visualized the localization of puromycin, Biotin-As, and aggresome in the cells. Scale bar, 25 μm. **B** The NB4 cells were treated with 1 μM Biotin-As for 4 h, and then 20 μM puromycin was added for another 30 min. Cell fractions were prepared for the Co-IP assays using the streptavidin magnetic beads and indicated antibodies. **C** Immunoblot of indicated proteins in the NB4 cells at 0, 4, 8, 12, and 24 h with 0.5 or 2 μM ATO treatment. **D** The NB4 cells were pre-treated with 0.5 μM PERKi (GSK2656157) or 10 μM GCN2iB for 1 h, and then 2 μM ATO was added for another 4 h. Immunoblot of indicated proteins in the NB4 cells.

untreated group, suggesting that arsenic induced more nascent polypeptides damage (Fig. 4H).

Based on the role of p97 in degrading damaged proteins, we investigated whether the sensitivity of NB4 to ATO could be increased with p97 inhibitors. We employed a p97 inhibitor NMS873 to pre-treat NB4 cells for 1 h and then indicated doses of ATO were added for the indicated time. The results showed that combination treatment could suppress protein synthesis more effectively than ATO alone and NMS873 enhanced the sensitivity of NB4 to ATO (Fig. 4I and Supplementary Fig. S7).

ATO and NMS873 have a synergistic effect on non-APL AML

Next, we explored the combined effect of ATO and NMS873 on non-APL AML. CCK-8 assay was used to detect cell viability after treatment with drugs for 72 h and Annexin V was used to detect cell apoptosis. The results indicated that NMS873 treatment could increase the sensitivity of Kasumi-1 to ATO, with a CI value of 0.36 when both ATO and NMS873 were at 1 μM (Fig. 5A, B), signifying a synergistic effect [54]. Similar results were observed for MOLM-13 and MV4-11 (Supplementary Fig. S8A–C). Protein aggregation analysis on Kasumi-1 and MOLM-13 revealed that the combination of ATO and NMS873 induced more protein aggregation (Fig. 5C and Supplementary Fig. S8D), indicative of increased production of damaged proteins.

Our previous results demonstrated that a lethal dose of ATO could induce severe ribosome stalling, activating JNK in NB4. Therefore, we studied the JNK activation in different AML cell lines. We found that the JNK pathway in Kasumi-1, MOLM-13, and MV4-11 was activated when treated by ATO combined with NMS873 (Fig. 5D and Supplementary Fig. S8E). Meanwhile, p-eIF2α and ATF4 were activated in Kasumi-1 under combination drug treatment (Fig. 5D), suggesting increased stress, resembling the impact of a lethal dose of ATO on NB4 cells. Furthermore, ZAKα activation was observed in Kasumi-1 under ATO and NMS873 treatment (Fig. 5E), indicating that combined treatment induced more ribosome stalling, activating the JNK pathway. To confirm the combination effect, we conducted p97 knockdown, which promoted apoptosis induced by ATO (Fig. 5F, G).

In addition to non-APL AML cell lines, we also explored the effect on patient AML cells ex vivo. Firstly, we confirmed that combination treatment had no significant effect on normal peripheral blood mononuclear cell apoptosis, although it seemed to induce more apoptosis (Fig. 5H). Next, we demonstrated that ATO combined with NMS873 could induce patient AML cell death (Fig. 5I), emphasizing the effect on non-APL AML.

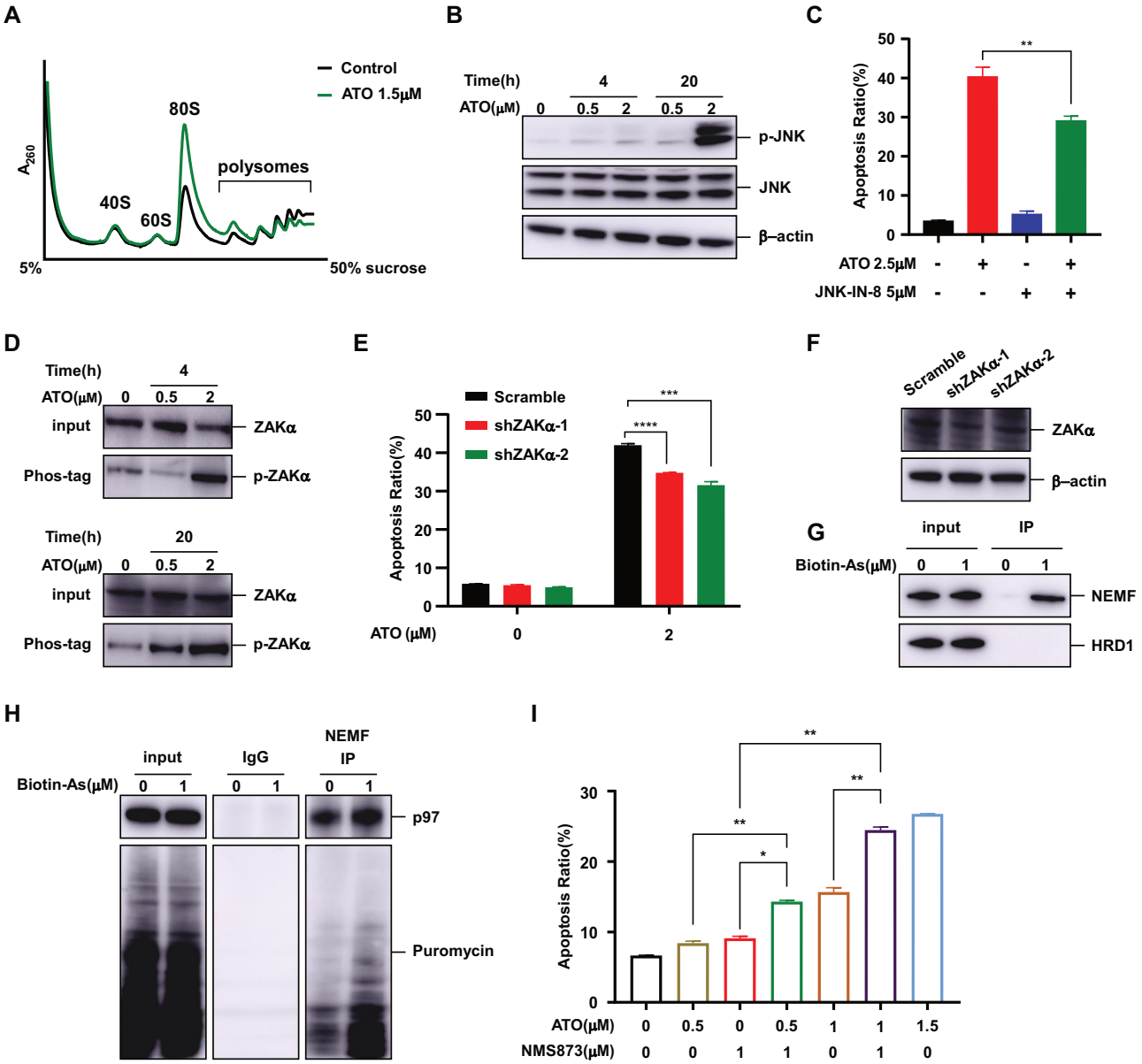

Fig. 4 ATO causes ribosome stalling and p97 inhibitor increases the sensitivity of APL to ATO. A Polysome profiles from NB4 cells with or without 1.5 μM ATO treatment for 6 h. **B** Immunoblot of indicated proteins in the NB4 cells at 0, 4, 20 h with 0.5 or 2 μM ATO treatment. **C** NB4 cells were pre-treated with 5 μM JNK inhibitor (JNK-IN-8) for 1 h, and then 2.5 μM ATO was added for another 24 h. Apoptosis was detected by flow cytometry. **D** Immunoblot of ZAKα and p-ZAKα in the NB4 cells at 4 or 20 h with 0.5 or 2 μM ATO treatment. The phosphorylated proteins in the cell lysate were enriched by Phos-tag™ Agarose. **E** The apoptosis ratio of ZAKα-knockdown NB4 cells with or without ATO treatment for 24 h. **F** Immunoblot of ZAKα in the ZAKα-knockdown NB4 cells. **G** The NB4 cells were treated with 1 μM Biotin-As for 4 h, and then cell fractions were prepared for the Co-IP assays using the streptavidin magnetic beads and indicated antibodies. **H** The NB4 cells were treated with 1 μM Biotin-As for 4 h, and then 20 μM puromycin was added for another 30 min. Cell fractions were prepared for the Co-IP assays using the NEMF, p97, and puromycin antibodies. **I** The NB4 cells were pre-treated with or without 1 μM NMS873 for 1 h and then indicated doses of ATO were added for another 24 h. The apoptosis ratio was detected by flow cytometry. Two-tailed Student *t* test, $^{*}P < 0.05$, $^{**}P < 0.01$, $^{***}P < 0.001$, $^{****}P < 0.0001$. Error bars reflect ± SEM of three independent experiments.

Effectiveness of ATO and NMS873 in vivo

Our in vitro data revealed a synergy between ATO and NMS873. We next investigated the effect of NMS873 and ATO in vivo. A Kasumi-1 xenograft model was generated by injecting Luciferase-GFP-Kasumi-1 tumor cells into the NSG mice intravenously (Fig. 6A). Tumor growth was monitored by the quantitative imaging system. We found that single-drug treatments and untreated mice showed no significant inhibition of leukemia progression, whereas combination drug treatment notably delayed tumor progression (Fig. 6B). The median survival time of mice treated with vehicle, ATO, NMS873, or the combination was 51, 54, 60, and 94 days, respectively (Fig. 6C). Thus, in vivo, the combination of ATO and the p97 inhibitor NMS873 exhibited an excellent inhibitory effect on ATO-low-sensitive AML cells.

DISCUSSION

In this study, we have illustrated the capability of ATO to induce apoptosis in APL cells by targeting nascent polypeptides and activating the ZAKα–JNK pathway. Our findings reveal distinct cellular responses depending on the dosage of ATO administered. Nonlethal doses of ATO activate the GCN2–ATF4

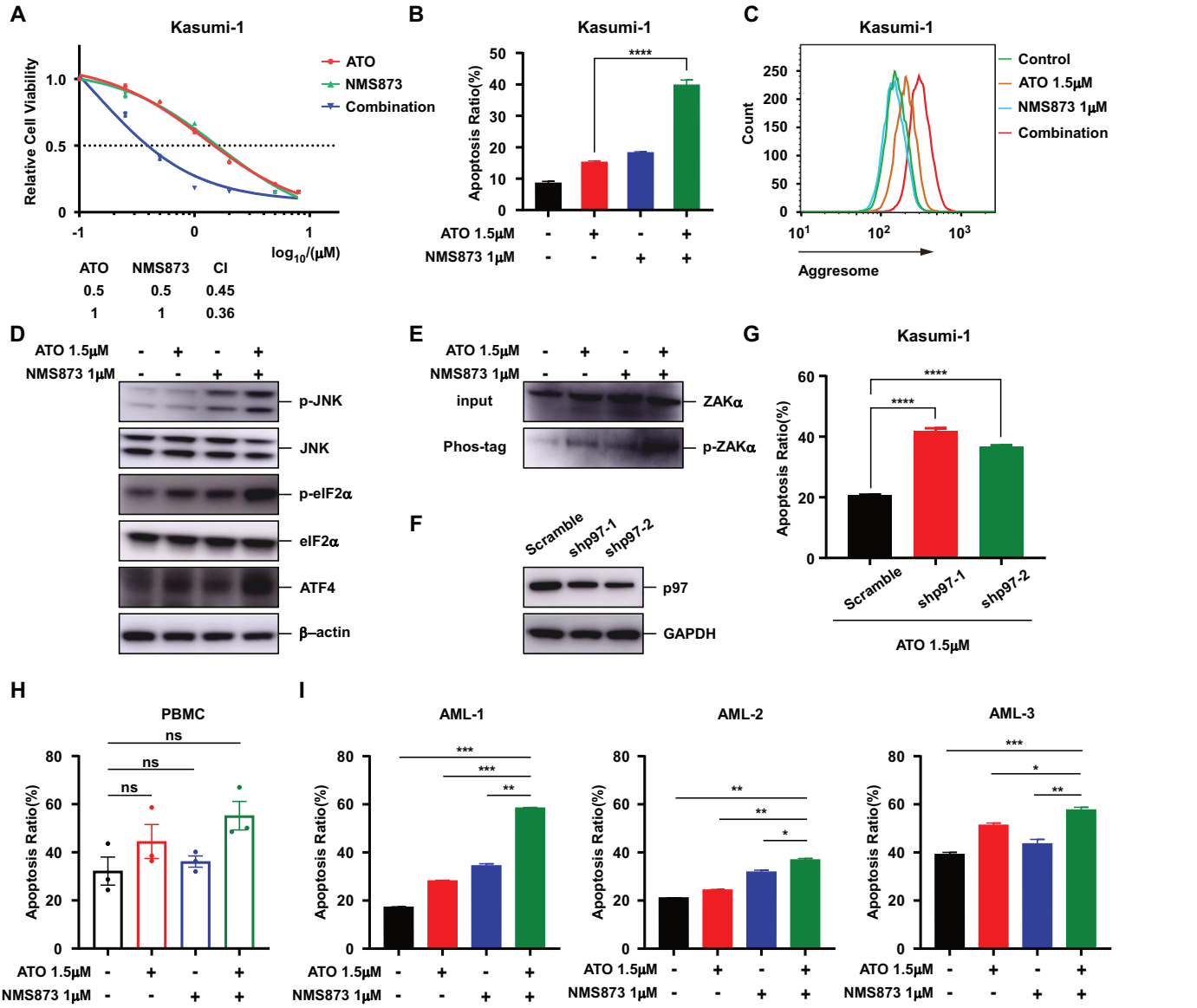

Fig. 5 ATO and NMS873 have a synergistic effect on non-APL AML. A Cell viability of Kasumi-1 with ATO, NMS873, or combination treatment (ATO: NMS873 = 1:1) after 72 h. The CI of different combination groups was quantified by Compusyn. **B** The Kasumi-1 cells were pre-treated with 1 μM NMS873 for 1 h, and then 1.5 μM ATO was added for another 24 h. The apoptosis ratio was detected by flow cytometry. **C** The Kasumi-1 cells were pre-treated with 1 μM NMS873 for 1 h, and then 1.5 μM ATO was added for another 12 h. The aggresome was detected by flow cytometry using the Enzo PROTEOSTAT® Aggresome detection kit. **D** The Kasumi-1 cells were pre-treated with 1 μM NMS873 for 1 h, and then 1.5 μM ATO was added for another 4 h. Immunoblot of indicated proteins in the Kasumi-1 cells. **E** Immunoblot of ZAKα and p-ZAKα in the Kasumi-1 cells at 4 h with 1.5 μM ATO, 1 μM NMS873, or combination treatment. The phosphorylated proteins in the cell lysate were enriched by Phos-tag™ Agarose. **F** Immunoblot of p97 in the p97-knockdown Kasumi-1 cells. **G** The apoptosis ratio of p97-knockdown Kasumi-1 cells after treatment with 1.5 μM ATO for 24 h. **H** The apoptosis ratio of PBMC from three healthy donors with 1.5 μM ATO, 1 μM NMS873, or combination treatment for 72 h. **I** The apoptosis ratio of AML cells from three AML patients with 1.5 μM ATO, 1 μM NMS873, or combination treatment for 24 h. Two-tailed Student *t* test, $^{*}P < 0.05$, $^{**}P < 0.01$, $^{***}P < 0.001$, $^{****}P < 0.0001$, the ns indicate no significant difference. Error bars reflect ± SEM of three independent experiments.

pathway, enabling APL cells to cope with stress during prolonged exposure and ultimately leading to cell survival. Conversely, the lethal dose of ATO triggers rapid activation of GCN2–ATF4, followed by activation of the JNK pathway during extended treatment, ultimately leading to apoptosis. In addition, our study demonstrates that ATO induces ribosome stalling. Up to now, ATO alone fails to confer any survival benefit to non-APL AML patients and exhibits limited efficacy when used in combination with other agents [7–9]. Thus, there is a need for us to explore a new agent combined with ATO to treat non-APL AML. Moreover, our study also highlights the importance of clearing ATO-induced damaged nascent polypeptides through p97-associated RQC. Therefore, we employ a p97 inhibitor in combination with ATO for non-APL AML treatment, leading to promising results. Interestingly, the JNK pathway is activated on non-APL AML when treated with combination drugs, mirroring the effects observed with lethal doses of ATO in APL (Fig. 7).

Here, we present a novel mechanism through which ATO induces APL cell death by targeting the nascent polypeptides. Given the inconsistencies between apoptosis and PML-RARα protein degradation, we verified that the degradation of fusion

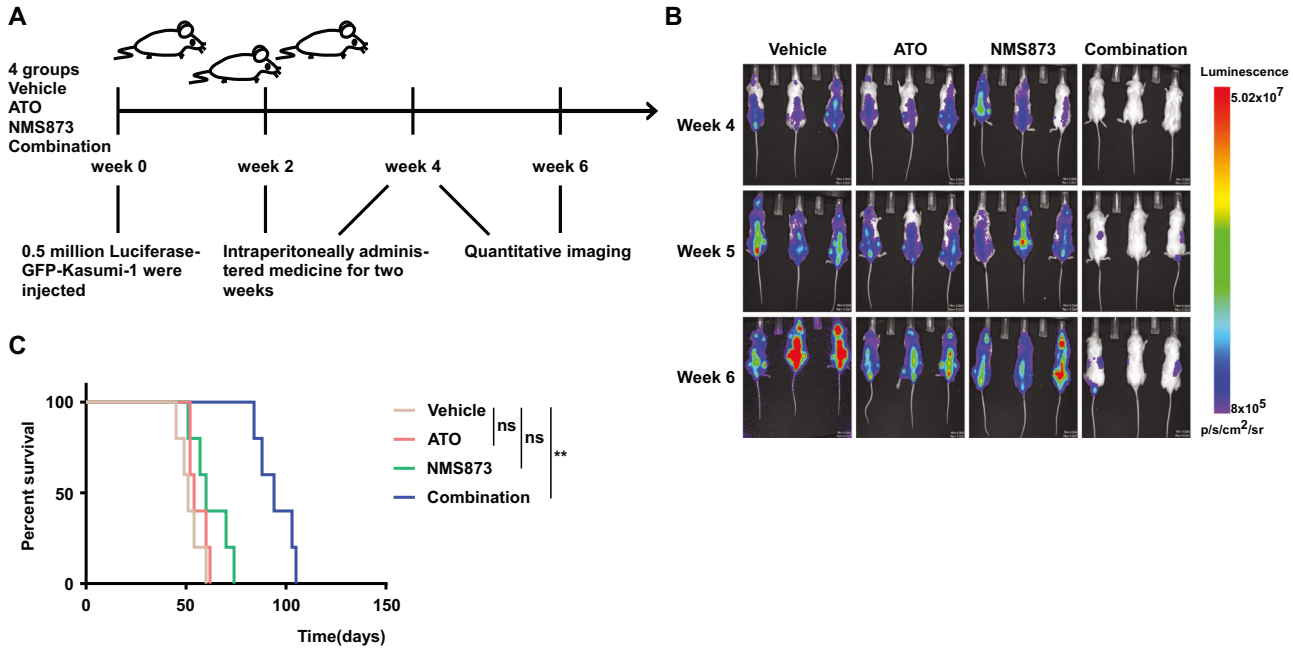

Fig. 6 Effectiveness of ATO and NMS873 in vivo. A In total, 0.5×10^6 Luciferase-GFP-Kasumi-1 tumor cells were injected into NSG mice (6 weeks, female) intravenously. Mice were allocated randomly into different experimental groups (4 groups, $n = 5$) and then intraperitoneally administered 2 mg/kg ATO or 2.6 mg/kg NMS873, respectively, or in combination, every other day for two weeks, beginning 14 days after the xenograft. Schematic for the different treatment strategies on the Lucuferase-GFP-Kasumi-1 cells was shown. **B** Representative bioluminescence images of tumor growth over time. **C** The survival curve of mice post-transplantation was shown. Mouse survival was monitored regularly and statistically analyzed using a long-rank test, $^{**}P < 0.01$, the ns indicate no significant difference.

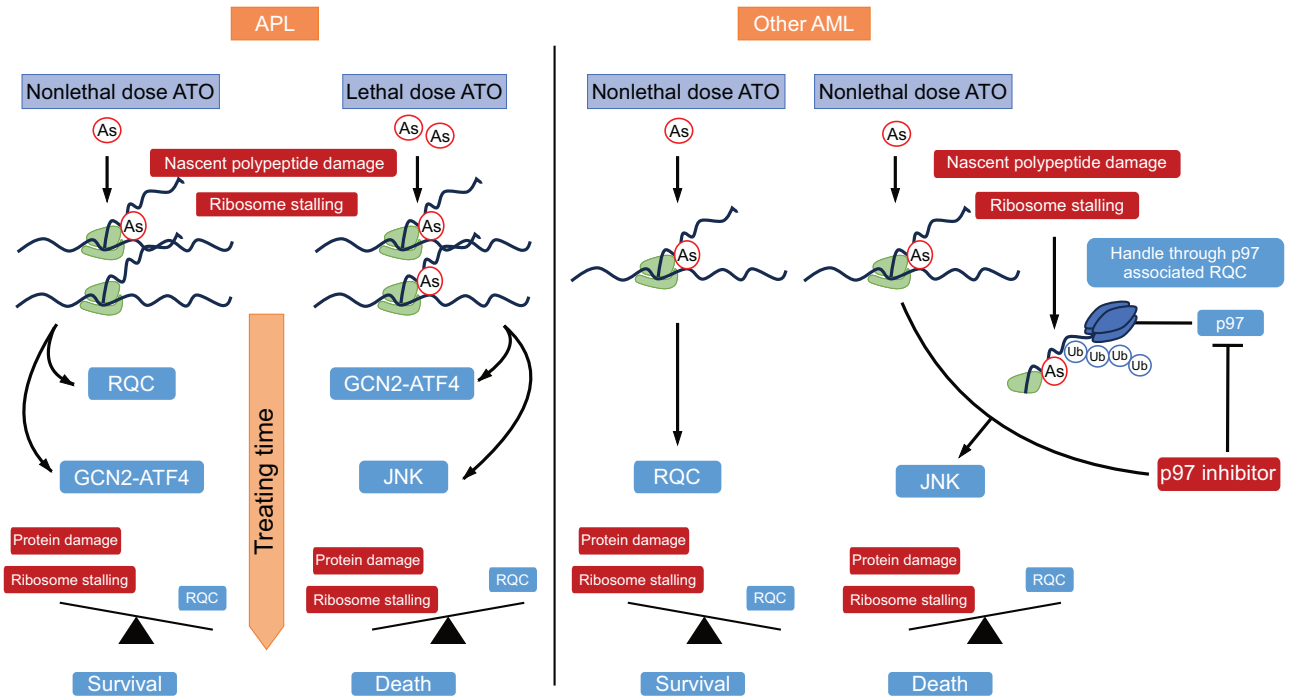

Fig. 7 The Schematic for the mechanism of ATO or ATO combined with p97 inhibitor induces AML death. ATO induces APL cell death by targeting nascent polypeptides and activating the ZAKα-JNK pathway. Nonlethal doses of ATO activate the GCN2–ATF4 pathway, enabling APL cells to cope with stress during prolonged exposure and ultimately leading to cell survival. Conversely, the lethal dose of ATO triggers rapid activation of GCN2–ATF4, followed by activation of the JNK pathway during extended treatment, ultimately leading to apoptosis. Moreover, ATO-induced damaged nascent polypeptides need to be cleared through p97-associated RQC. A nonlethal dose of ATO-induced stress in non-APL AML could be handled through RQC, resulting in cell survival. However, the p97 inhibitor combined with ATO can activate the JNK pathway in non-APL AML, resulting in cell death.

proteins is insufficient to cause tumor cell death, nor was the ROS upregulation. Through comparison with the wild-type NB4, we found an enrichment of cysteine-rich peptides in the NB4-AR cells. Previous studies have shown that mature cysteine-rich proteins, such as hexokinase-2 [19], thioredoxin reductase [55], and Pyruvate Dehydrogenase [56, 57] are direct or indirect targets of arsenic. These functional proteins sustain the survival of tumor cells and their significant inhibition by arsenic may result in cell death [19, 55–57]. However, little attention has been paid to nascent polypeptides damage induced by ATO. Protein synthesis emerges as a pivotal factor influencing protein homeostasis [44]. Based on the protein synthesis of different AML cells and their sensitivity to ATO, we hypothesized a correlation between ATO-induced cell death and protein synthesis. This suspicion was substantiated by our experiments demonstrating that CHX and 4EGI-1 inhibit cell apoptosis induced by ATO. Notably, not all protein synthesis inhibitors yielded the same effect as CHX or 4EGI-1. Instead, puromycin promoted ATO-induced cell apoptosis, leading us to focus on the nascent polypeptides damage. The protein synthesis rate in hematopoietic stem cells is strictly controlled, and the increase in protein synthesis may result in leukemia [58]. Thus, protein homeostasis becomes the most ideal target for the treatment of AML.

The protein homeostasis is sustained by a series of responses, including UPR and ISR [21, 22, 26, 27]. Studies have shown that arsenic can induce apoptosis in various cells through ER stress or UPR [31–35]. Little attention has been paid to ISR induced by ATO. In our investigation, we did not observe the activation of ATF6α and XBP1s. However, p-eIF2α and ATF4 could be activated in NB4 by treatment with a lethal dose of ATO. Furthermore, we found that GCN2, but not PERK, was activated, suggesting that ATO treatment induces ISR rather than UPR, which is a vital addition to existing research [31–35]. In addition, we also demonstrated that ATO induced ribosome stalling and activated the JNK pathway, establishing the association among ribosome stalling, GCN2, and JNK activation in NB4 under ATO treatment. These findings were in accord with the concept that ribosome stalling triggered the JNK and GCN2-mediated stress response pathways [30, 48, 49]. However, due to the partial inhibition of apoptosis by JNK inhibition or ZAKα knockdown, there must be other mechanisms for ATO-induced apoptosis. ATO-induced stress is complex. For example, ATO can also induce ROS and PML-RARα protein degradation. Neither the degradation of the fusion protein nor the increase of ROS can fully explain ATO-induced death, just like the ZAKα–JNK pathway.

In addition, damaged proteins require clearance through ERAD or RQC [37, 38]. Our data revealed that ATO-induced damaged proteins interacted with RQC-associated proteins. The pivotal role of p97 in RQC was evident, and our study demonstrated that the p97 inhibitor NMS873 had a synergistic effect with ATO on non-APL AML, particularly in the case of Kasumi-1 cells. Up to now, a second-generation inhibitor of p97, CB-5339, has been tested in acute myeloid leukemia or myelodysplastic syndrome (NCT04402541), highlighting its potential application in clinical settings.

In summary, our study provides new insights into the mechanism of ATO-induced APL cell death and discovers the apoptosis of AML cells induced by ATO is related to nascent polypeptides damage and the ZAKα-JNK pathway activation. Moreover, p97 inhibitors combined with ATO show synergistic lethal ability on non-APL AML cells, which could be a clinical reference and give new prospects for further study. However, several limitations of our study should be mentioned. First, we used NAC and GSH to validate our hypothesis that arsenic primarily acts by targeting the sulfhydryl group of cysteine in proteins. However, NAC and GSH are also ROS scavengers, and their inhibition of ATO-induced apoptosis may support the idea that ATO induces apoptosis via ROS. Therefore, more appropriate reagents or methods may be needed to support our hypothesis. Next, based on the rapid activation of ZAKα but not JNK at lethal doses of ATO, we think that sufficient p-ZAKα is required for p-JNK activation. Because 20 h of nonlethal dose ATO treatment activated ZAKα but not JNK. However, how much p-ZAKα is sufficient to activate JNK to induce cell death remains unclear. Third, we confirmed that combination treatment had no significant effect on normal peripheral blood mononuclear cell apoptosis, although it seemed to induce more apoptosis. Thus, whether normal cells are protected from the effect of ATO due to their low protein synthesis rate needs to be carefully explored. In addition, more patients' AML cells were needed to demonstrate the killing effect of combination treatment. Furthermore, we employed the Kasumi-1 cell line as our target cell for exploring the effect of combination drugs. The reason why Kasumi-1 was more sensitive to combination treatment remains to be further explored. Next, we did not elucidate the direct interaction between ATO-induced nascent polypeptides damage and ribosome stalling. Studies have shown that abnormal nascent peptide chains induced ribosome stalling [59], but the precise mechanism through which ATO-induced damage to nascent polypeptides influences ribosome stalling requires further exploration.

DATA AVAILABILITY

The datasets generated and analyzed during the current study are available from the corresponding author upon reasonable request.

REFERENCES

1. Döhner H, Weisdorf DJ, Bloomfield CD. Acute myeloid leukemia. New Engl J Med. 2015;373:1136–52.
2. Kantarjian H, Kadia T, DiNardo C, Daver N, Borthakur G, Jabbour E, et al. Acute myeloid leukemia: current progress and future directions. Blood Cancer J. 2021;11:41.
3. Chen Z, Chen SJ. Poisoning the devil. Cell. 2017;168:556–60.
4. Wang ZY, Chen Z. Acute promyelocytic leukemia: from highly fatal to highly curable. Blood. 2008;111:2505–15.
5. Lo-Coco F, Avvisati G, Vignetti M, Thiede C, Orlando SM, Iacobelli S, et al. Retinoic acid and arsenic trioxide for acute promyelocytic leukemia. New Engl J Med. 2013;369:111–21.
6. Shen ZX, Shi ZZ, Fang J, Gu BW, Li JM, Zhu YM, et al. All-trans retinoic acid/As2O3 combination yields a high quality remission and survival in newly diagnosed acute promyelocytic leukemia. Proc Natl Acad Sci USA. 2004;101:5328–35.
7. Parmar S, Rundhaugen LM, Boehlke L, Riley M, Nabhan C, Raji A, et al. Phase II trial of arsenic trioxide in relapsed and refractory acute myeloid leukemia, secondary leukemia and/or newly diagnosed patients at least 65 years old. Leuk Res. 2004;28:909–19.
8. Aldoss I, Mark L, Vrona J, Ramezani L, Weitz I, Mohrbacher AM, et al. Adding ascorbic acid to arsenic trioxide produces limited benefit in patients with acute myeloid leukemia excluding acute promyelocytic leukemia. Ann Hematol. 2014;93:1839–43.
9. Dilda PJ, Hogg PJ. Arsenical-based cancer drugs. Cancer Treat Rev. 2007;33:542–64.
10. Jiang Y, Shen X, Zhi F, Wen Z, Gao Y, Xu J, et al. An overview of arsenic trioxide-involved combined treatment algorithms for leukemia: basic concepts and clinical implications. Cell Death Discov. 2023;9:266.
11. Lallemand-Breitenbach V, Jeanne M, Benhenda S, Nasr R, Lei M, Peres L, et al. Arsenic degrades PML or PML-RARalpha through a SUMO-triggered RNF4/ubiquitin-mediated pathway. Nat Cell Biol. 2008;10:547–55.
12. Zhang XW, Yan XJ, Zhou ZR, Yang FF, Wu ZY, Sun HB, et al. Arsenic trioxide controls the fate of the PML-RARalpha oncoprotein by directly binding PML. Science. 2010;328:240–3.
13. Liu JX, Zhou GB, Chen SJ, Chen Z. Arsenic compounds: revived ancient remedies in the fight against human malignancies. Curr Opin Chem Biol. 2012;16:92–8.
14. de Thé H, Chen Z. Acute promyelocytic leukaemia: novel insights into the mechanisms of cure. Nat Rev Cancer. 2010;10:775–83.
15. de Thé H, Pandolfi PP, Chen Z. Acute promyelocytic leukemia: a paradigm for oncoprotein-targeted cure. Cancer Cell. 2017;32:552–60.

16. Sumi D, Shinkai Y, Kumagai Y. Signal transduction pathways and transcription factors triggered by arsenic trioxide in leukemia cells. Toxicol Appl Pharm. 2010;244:385–92.
17. Jing Y, Dai J, Chalmers-Redman RM, Tatton WG, Waxman S. Arsenic trioxide selectively induces acute promyelocytic leukemia cell apoptosis via a hydrogen peroxide-dependent pathway. Blood. 1999;94:2102–11.
18. Morales AA, Gutman D, Cejas PJ, Lee KP, Boise LH. Reactive oxygen species are not required for an arsenic trioxide-induced antioxidant response or apoptosis. J Biol Chem. 2009;284:12886–95.
19. Zhang HN, Yang L, Ling JY, Czajkowsky DM, Wang JF, Zhang XW, et al. Systematic identification of arsenic-binding proteins reveals that hexokinase-2 is inhibited by arsenic. Proc Natl Acad Sci USA. 2015;112:15084–9.
20. Shen S, Li XF, Cullen WR, Weinfeld M, Le XC. Arsenic binding to proteins. Chem Rev. 2013;113:7769–92.
21. Oakes SA, Papa FR. The role of endoplasmic reticulum stress in human pathology. Annu Rev Pathol. 2015;10:173–94.
22. Walter P, Ron D. The unfolded protein response: from stress pathway to homeostatic regulation. Science. 2011;334:1081–6.
23. Wang M, Kaufman RJ. Protein misfolding in the endoplasmic reticulum as a conduit to human disease. Nature. 2016;529:326–35.
24. Lin JH, Li H, Yasumura D, Cohen HR, Zhang C, Panning B, et al. IRE1 signaling affects cell fate during the unfolded protein response. Science. 2007;318:944–9.
25. Tabas I, Ron D. Integrating the mechanisms of apoptosis induced by endoplasmic reticulum stress. Nat Cell Biol. 2011;13:184–90.
26. Pakos-Zebrucka K, Koryga I, Mnich K, Ljujic M, Samali A, Gorman AM. The integrated stress response. EMBO Rep. 2016;17:1374–95.
27. Nwosu GO, Powell JA, Pitson SM. Targeting the integrated stress response in hematologic malignancies. Exp Hematol Oncol. 2022;11:94.
28. Berlanga JJ, Ventoso I, Harding HP, Deng J, Ron D, Sonenberg N, et al. Antiviral effect of the mammalian translation initiation factor 2alpha kinase GCN2 against RNA viruses. EMBO J. 2006;25:1730–40.
29. Wu CC, Peterson A, Zinshteyn B, Regot S, Green R. Ribosome collisions trigger general stress responses to regulate cell fate. Cell. 2020;182:404–16.e14.
30. Yan LL, Zaher HS. Ribosome quality control antagonizes the activation of the integrated stress response on colliding ribosomes. Mol Cell. 2021;81:614–28.e4.
31. Weng CY, Chiou SY, Wang L, Kou MC, Wang YJ, Wu MJ. Arsenic trioxide induces unfolded protein response in vascular endothelial cells. Arch Toxicol. 2014;88:213–26.
32. Binet F, Chiasson S, Girard D. Arsenic trioxide induces endoplasmic reticulum stress-related events in neutrophils. Int Immunopharmacol. 2010;10:508–12.
33. Oh RS, Pan WC, Yalcin A, Zhang H, Guilarte TR, Hotamisligil GS, et al. Functional RNA interference (RNAi) screen identifies system A neutral amino acid transporter 2 (SNAT2) as a mediator of arsenic-induced endoplasmic reticulum stress. J Biol Chem. 2012;287:6025–34.
34. Yen CC, Ho TJ, Wu CC, Chang CF, Su CC, Chen YW, et al. Inorganic arsenic causes cell apoptosis in mouse cerebrum through an oxidative stress-regulated signaling pathway. Arch Toxicol. 2011;85:565–75.
35. Chiu HW, Tseng YC, Hsu YH, Lin YF, Foo NP, Guo HR, et al. Arsenic trioxide induces programmed cell death through stimulation of ER stress and inhibition of the ubiquitin-proteasome system in human sarcoma cells. Cancer Lett. 2015;356:762–72.
36. Pilla E, Schneider K, Bertolotti A. Coping with protein quality control failure. Annu Rev Cell Dev Biol. 2017;33:439–65.
37. Buchberger A, Bukau B, Sommer T. Protein quality control in the cytosol and the endoplasmic reticulum: brothers in arms. Mol Cell. 2010;40:238–52.
38. Joazeiro CAP. Ribosomal stalling during translation: providing substrates for ribosome-associated protein quality control. Annu Rev Cell Dev Biol. 2017;33:343–68.
39. Hwang J, Qi L. Quality control in the endoplasmic reticulum: crosstalk between ERAD and UPR pathways. Trends Biochem Sci. 2018;43:593–605.
40. Eisenack TJ, Trentini DB. Ending a bad start: triggers and mechanisms of co-translational protein degradation. Front Mol Biosci. 2022;9:1089825.
41. Verma R, Oania RS, Kolawa NJ, Deshaies RJ. Cdc48/p97 promotes degradation of aberrant nascent polypeptides bound to the ribosome. Elife. 2013;2:e00308.
42. Joazeiro CAP. Mechanisms and functions of ribosome-associated protein quality control. Nat Rev Mol Cell Biol. 2019;20:368–83.
43. Lyublinskaya OG, Ivanova JS, Pugovkina NA, Kozhukharova IV, Kovaleva ZV, Shatrova AN, et al. Redox environment in stem and differentiated cells: a quantitative approach. Redox Biol. 2017;12:758–69.
44. Hipp MS, Kasturi P, Hartl FU. The proteostasis network and its decline in ageing. Nat Rev Mol Cell Biol. 2019;20:421–35.
45. Aviner R. The science of puromycin: from studies of ribosome function to applications in biotechnology. Comput Struct Biotechnol J. 2020;18:1074–83.
46. Vattem KM, Wek RC. Reinitiation involving upstream ORFs regulates ATF4 mRNA translation in mammalian cells. Proc Natl Acad Sci USA. 2004;101:11269–74.
47. Bertolotti A, Zhang Y, Hendershot LM, Harding HP, Ron D. Dynamic interaction of BiP and ER stress transducers in the unfolded-protein response. Nat Cell Biol. 2000;2:326–32.
48. Vind AC, Snieckute G, Blasius M, Tiedje C, Krogh N, Bekker-Jensen DB, et al. ZAKα recognizes stalled ribosomes through partially redundant sensor domains. Mol Cell. 2020;78:700–13.e7.
49. Snieckute G, Genzor AV, Vind AC, Ryder L, Stoneley M, Chamois S, et al. Ribosome stalling is a signal for metabolic regulation by the ribotoxic stress response. Cell Metab. 2022;34:2036–46.e8.
50. Dang Y, Kedersha N, Low WK, Romo D, Gorospe M, Kaufman R, et al. Eukaryotic initiation factor 2alpha-independent pathway of stress granule induction by the natural product pateamine A. J Biol Chem. 2006;281:32870–8.
51. Ashe MP, De Long SK, Sachs AB. Glucose depletion rapidly inhibits translation initiation in yeast. Mol Biol Cell. 2000;11:833–48.
52. Davison K, Mann KK, Waxman S, Miller WH Jr. JNK activation is a mediator of arsenic trioxide-induced apoptosis in acute promyelocytic leukemia cells. Blood. 2004;103:3496–502.
53. Defenouillère Q, Yao Y, Mouaikel J, Namane A, Galopier A, Decourty L, et al. Cdc48-associated complex bound to 60S particles is required for the clearance of aberrant translation products. Proc Natl Acad Sci USA. 2013;110:5046–51.
54. Chou TC. Theoretical basis, experimental design, and computerized simulation of synergism and antagonism in drug combination studies. Pharm Rev. 2006;58:621–81.
55. Lu J, Chew EH, Holmgren A. Targeting thioredoxin reductase is a basis for cancer therapy by arsenic trioxide. Proc Natl Acad Sci USA. 2007;104:12288–93.
56. Bergquist ER, Fischer RJ, Sugden KD, Martin BD. Inhibition by methylated organo-arsenicals of the respiratory 2-oxo-acid dehydrogenases. J Organomet Chem. 2009;694:973–80.
57. Samikkannu T, Chen CH, Yih LH, Wang AS, Lin SY, Chen TC, et al. Reactive oxygen species are involved in arsenic trioxide inhibition of pyruvate dehydrogenase activity. Chem Res Toxicol. 2003;16:409–14.
58. Signer RA, Magee JA, Salic A, Morrison SJ. Haematopoietic stem cells require a highly regulated protein synthesis rate. Nature. 2014;509:49–54.
59. Ramu H, Vázquez-Laslop N, Klepacki D, Dai Q, Piccirilli J, Micura R, et al. Nascent peptide in the ribosome exit tunnel affects functional properties of the A-site of the peptidyl transferase center. Mol Cell. 2011;41:321–30.

ACKNOWLEDGEMENTS

The authors thank Dr. Junmin Li at Ruijin Hospital for his assistance in acquiring the AML cells from patients. The authors acknowledge the contributions to this study of the patients.

AUTHOR CONTRIBUTIONS

SX designed and performed most of the experiments, analyzed the data, and wrote the draft manuscript; HL, SZ, and ZC performed some experiments and revised the manuscript; RW, YS, JL, and CL constructed NB4-AR cell and analyzed RNA-seq data; WZ, HX, RX, YW, and MW revised the partial manuscript; XX, YW, YY, and ZH provided expertise and analyzed the data; ZX and HL contributed grant support, designed the entire project, and wrote the manuscript. All authors discussed the results and commented on the manuscript.

FUNDING

This work was supported by the National Natural Science Foundation of China (82470154, 82100154, 82200245, 82104447, and 82270175), the Open Project Program of the National Research Center for Translational Medicine at Shanghai (TMSZ-2020-204 and NRCTM(SH)-2021-09), the Natural Science Foundation of Fujian Province of China (2021J02040), the Joint Funds for the Innovation of Science and Technology of Fujian Province (2023Y9173), the Collaborative Innovation Center of Hematology, and the Samuel Waxman Cancer Research Foundation.

COMPETING INTERESTS

The authors declare no competing interests.

ETHICS APPROVAL AND CONSENT TO PARTICIPATE

The human study was approved by the Ethics Committee of Ruijin Hospital, Shanghai Jiao Tong University School of Medicine. Written informed consent was obtained from each participant. The study was performed in accordance with the Declaration of Helsinki. Animal care and sacrifice were conducted according to methods

approved by the Animal Care and Use Committee, the Center for Animal Experiments of Shanghai Jiao Tong University.

ADDITIONAL INFORMATION

Supplementary information The online version contains supplementary material available at https://doi.org/10.1038/s41417-024-00818-z.

Correspondence and requests for materials should be addressed to Shufeng Xie, Zhenshu Xu or Han Liu.

Reprints and permission information is available at http://www.nature.com/reprints

Publisher's note Springer Nature remains neutral with regard to jurisdictional claims in published maps and institutional affiliations.